Official Dental Journal of Suez Canal University
DENTAL SCIENCE Updates
Print ISSN 2636-3836
Online ISSN 2636-3844
www.dsujournals.ekb.eg
DSU — Vol. 4, No. 2, September (2023) — PP. 313:328

EFFECT OF THYMOQUINONE ON SKELETAL MUSCLE REGENERATION AND INNERVATION IN INDUCED DEGENERATION OF THE HAMSTER BUCCAL POUCH

Asmaa Mohammed Fahmy Abd El-Wahed [1], Ahmed Mohammed Moheb El-din Korraah [2], Fadia Mostafa Attia [3], and Magda Mohammed Aly Hassan[4]

DOI: 10.21608/dsu.2023.187143.1154
Manuscript ID: DSU-2301-1154

KEYWORDS

7,12-Dimethylbenz[a] anthracene; Muscle regeneration; Neurofilament heavy chain; Pax-7; Thymoquinone.

- E-mail address: asmaa_elwahed@dent.suez.edu.eg

1. Assistant lecturer in Oral Pathology Department, Faculty of Dentistry, Suez Canal University.
2. Lecturer of Oral Pathology, Faculty of Dentistry, Ismailia, Suez Canal University.
3. Professor of Clinical Pathology, Head of Clinical Pathology Department, Faculty of Medicine, Suez Canal University.
4. Professor of Oral Pathology, Faculty of Dentistry, Ismailia, Suez Canal University.

ABSTRACT

Introduction: Thymoquinone (TQ) has myogenic and neurogenic properties. **Aim**: This research aimed to study the effect of TQ on skeletal muscle regeneration and innervation in DMBA – induced degeneration of hamster buccal pouch (HBP). **Material and Methods**: 70 male golden Syrian hamsters were divided into 3 groups. Group A: (5) untreated animals. Group B: (5 animals), their left pouches were painted with 0.5% DMBA 3/week/6 weeks. Group C: (60 animals) was treated as group B, then divided equally into Group CI and Group CII: They received one and two i.p. TQ (0.1 mg/kg body weight) injection(s), respectively, then 5 animals from each subgroup were euthanized at 1, 2, 4, 7, 14, and 20 days. All pouches were surgically excised and processed for H&E, and immunohistochemistry stain of Pax-7 and neurofilament heavy chain (NFH). The obtained data were statistically analyzed. **Results:** The muscle layer' bulk of left pouches was progressively forming from 7 and 4 days after one and two TQ injection(s), respectively. Perivascular mononuclear cells (MNCs) were Pax-7 positive from the second and first day(s) to 14 and 7 days after one and two injection(s), as well the nuclei of mature muscle fibers (MFs) from 4 and 2 days to about 20 and 14 days after one and two TQ injection(s), respectively. The intensity of NFH IHC stain was progressively increased from the second and first day(s) after one and two TQ injection(s), respectively, as MFs membranes' plaques. **Conclusion**: TQ stimulated skeletal muscles' regeneration and re-innervation in HBPs.

INTRODUCTION

Skeletal muscle comprises a large percentage of the human body mass and formed of differentiated myofibers that have irreversibly left the cell cycle [(1)]. Muscle satellite cells (SCs), contribute to the growth and regeneration of postnatal muscle by fusing with damaged myofibers or producing new myofibers. Following injury of skeletal muscle, resident quiescent SCs enter the cell cycle and generate myoblasts that will participate in myofiber reconstitution or repair [(2)].

Skeletal muscle regeneration is affected by the balance between pro-and anti-inflammatory factors that determine fibrosis or repair of muscle fibres. Muscle regeneration occurs in five interrelated and time-dependent phases, namely, degeneration (necrosis), inflammation, regeneration, remodeling, and maturation/ functional repair[(3)]. The degeneration phase is characterized by necrosis and significant inflammation. From 3 to 14 days post-injury, clearance of cellular debris

and new fibers that express embryonic and neonatal myosin heavy chain (MyHC) are formed. The phase of remodeling is characterized by hyperplasia and hypertrophy that is regulated in part by the insulin growth factor-1 and transforming growth factor-β pathways. During final steps of muscle remodeling, the vasculature and innervation patterns are restored[4].

The study of classic rout of muscle regeneration depends on injection of cardiotoxin (CTX) in animals' muscle, mostly in rats or mice tibialis, plantaris' or soleus' muscles, then allowed these muscles to regenerate. CTX produces a local myonecrosis and stimulates muscle regeneration [5]. It was found that after few hours of CTX injection, neutrophils infiltrate the necrotic tissue. The phase of necrosis extends up to 2 days. While the inflammatory phase started at about 2-3 hours after CTX treatment and up to 4 days. Moreover, after 2 days, spindle-shaped mononucleated cells mixed with necrotic debris, leukocytes, and macrophages appear. The muscle regeneration phase was 2-14 days after CTX treatment. By 7–10 days after CTX injection, most of muscle bulk is restored. These regenerated MFs are smaller with centrally located myonuclei. The progressive maturation of regenerating myofibers occurs 10 to 15, with functional restoration and innervation from 15-20 days[5, 6]. The length of each phasedepends on the type of organism(e.g.,mouse, rat, and human), the extent of damage, type of muscle and the damage model used.

Pax7 is one of the paired-domain transcription factors (Pax-3 and Pax-7), plays a critical role for postnatal muscle formation, and induced during muscle regeneration and maturation [7].

Neurofilaments (NFs) are intermediate filaments (IF), present in dendrites, perikaryal (the cell body of a neuron), and abundant in axons. They are essential for the radial growth of axons during development; maintain axon caliber and the velocity of nerve conduction[8]. They are synthesized in the perikaryal, then quickly translocated into the axons, and assemble into filamentous structures[9]. Taken together, injured peripheral nerves and skeletal muscles have a remarkable ability for tissue regeneration [10].

The 7, 12-Dimethylbenz [a]-anthracene (DMBA) is a member of the polycyclic aromatic hydrocarbons (PAHs) that present in cigarette smoke. It is widely used as a model of PAHs to induce carcinogenesis in models specially the hamster buccal pouch (HBP), it is the most well-characterized system for analyzing the development of oral cancer (OC) [11].

Many phytochemicals have been proven to have important anti-cancerous effects with a good safety profile. Thymoquinone (TQ), the major active constituent of *Nigella sativa* Linnaeus (*NS*. L*)* is one of the promising medicinal agents. It has many biological effects as anti-oxidant, anti-inflammatory, anti-cancer, anti-microbial and immune-modulation[12].

In the HBP/DMBA model, the early few DMBA paintings resulted in reduction of HBPs' length to about 2cmwith necrosis of their distal ends. These painted pouches could not regain the full length even after cessation of DMBA painting [13, 14]. In a comparable study, it was reported that very small concentration and doses of TQ was able to induce regeneration of these pouches (nearly to normal length) in the DMBA-treated animals [15]. Moreover, TQ was found to prevent muscle and nerve tissues' damage during Dawley rat's ischemia-reperfusion (IR) of a lower limb [16].

The strong anti-inflammatory feature of TQ was reported by Algharyni *et al* (2019), when following TQ injection, TNF-α was cleared from inflammatory cells in the DMBA-painted pouches, and significantly increased in the blood, compared to untreated animals [15].

The present work used longer time of follow up for muscle regeneration than Algharyni *et al* study. It also studied the innervation of regenerated muscles.

MATERIAL AND METHODS

Approval of the Ethics Committee of Scientific Research, Faculty of Dentistry, Suez Canal University, has been obtained before starting the search (approval number: 265/2020).

Materials:

Carcinogen: The DMBA (Cat. No: D3254) was dissolved in heavy mineral oil (cat.No: M 3516) to get 0.5% solution. Both were purchased from Sigma Chemical Company, St. Louis, Mo, USA.

Thymoquinone (TQ) (C10H12O2):

Thymoquinone (Cat. No: D3254-1G) and propylene glycol (Cat. No: W2944004) were purchased from Sigma Chemical Company, St. Louis, Mo, USA.

Pax-7 and NFH kits for IHC stain:

The used dilution of either Pax-7 and NFH was 1:100. They were purchased from ABclonal technology, 500W Cummings Park, Ste. 6500 Woburn, Massachusetts 01801, USA. Pax-7 polyclonal rabbit antibodies (Rhabdomyosarcoma marker), (AB clonal, Catalog No. A12740) and monoclonal rabbit neurofilament antibody (NFH) (AB clonal, Catalog No. A19084).

Study design and animals grouping

Animals: This study was carried out on 70 male golden Syrian hamsters, weighing 100-120 grams, purchased from the Holding Company for Biological Products and Vaccines (VACERA), Helwan, Cairo, Egypt.

Sample size calculation: using the following formula: the confidence level 95%, and confidence interval of 2.5. Sample size = Z2 *P*(1-P) / C2, where: *Z=z Value, *P=Proportion of the population having the attribute and *C=Confidence interval, expressed as decimal.

By calculation, the sample size was equal to 5 animals per group, giving a total sample size of 70 animals.

The hamsters were divided into 3 groups. **Group A:** 5 untreated animals, served as negative control, and were euthanized at day zero. **Group B:** 5 animals were painted with DMBA (0.5% DMBA 3/week/6weeks), served as positive control. They were euthanized at second day of last painting. **Group C:** 60 animals were treated as group B, then divided into two sub-groups as follow: **Group CI:** 30 hamsters were given one i.p. injection with TQ (0.1 mg/kg body weight). **Group CII:** 30 hamsters were given two i.p. injections with TQ (0.1 mg/kg body weight) day after day. Five animals from each subgroup were euthanized at 1, 2, 4, 7, 14, and 20 days after the last TQ injection.

After euthanization (by inhalation of a lethal dose of ether as an ether-soaked piece of cotton in a tightly closed glass container), all pouches were surgically excised, fixed in 10% neutral buffered formalin and embedded in soft paraffin wax. Sections of 5μm were cut, processed for H&E and IHC stains of Pax-7 and NFH for light microscopic study.

The oral epithelial dysplasia (OED) was graded according to Bánóczy and Csiba [17] into:

- **Mild:** when an average of less than 3 dysplastic criteria were present (for each group).
- **Moderate**: when an average of 3-7 criteria were present (for each group).
- **Severe**: when an average of 7 or more criteria were present (for each group).
- **Carcinoma in situ**: when some or all criteria were distributed from top to bottom with intact basement membrane.

Immunohistochemical procedures:

Detection of Pax-7 and NFH IHC expression was done following the manufacturer's instructions.

Staining was detected using Ultravision detection system (Cat. No. TP-015-HD). The avidin–biotin complex (ABC) procedure (indirect technique) was used. The slides were diagnosed by two pathologists and photographed by Olympus E-330 Evolt Digital Photography camera using Image Analyzing System (Olympus BX50 Microscope). The semi-quantitative method was used to determine the intensity of immunohistochemical stain using the recent version of ImageJ software with IHC profiler plugin (1.48 version) (NIH, Bethesda, Maryland) (Java 1.8.9_66).

Immunohistochemical assessment:

The final score of both markers was set in a semi-quantitative way (high positive, positive, low positive or negative), and classified into four categories: negative =0, low positive =1, positive =2 and high positive =3, according to the intensity of staining [18].

The software Statistical Package for Social Sciences (SPSS) (version 12.0) was used for statistical analysis of IHC results. The mean difference is considered significant at $p \leq 0.05$ level. The IHC intensity of stain was expressed as mean ± standard deviation and was analyzed statistically using ANOVA test [19].

RESULTS

Clinical observation:

In group A (the negative control), animals appeared healthy and active, with normal appearing pouches (clear and whitish in color). The pouches measured about 5-6 cm. Whereas, animals from group B showed, perioral hair loss, exophytic masses and/or ulcers and severe inflammation of left side. The left pouches showed marked shortening to about 2 cm with severe inflammation, multiple ulcers and necrosis at the distal ends **(Figure 1)**. By end of the experiment and after one and two TQ injection(s), the left pouches measured about 4.5-5cm.

Histological findings:

Group A showed normal mucosa of both buccal pouches, i.e, thin keratinized squamous epithelium, no rete ridges, thin not inflamed collagenous lamina propria. The muscle fibres in the deeper layers are loosely arranged. On the other hand, group B

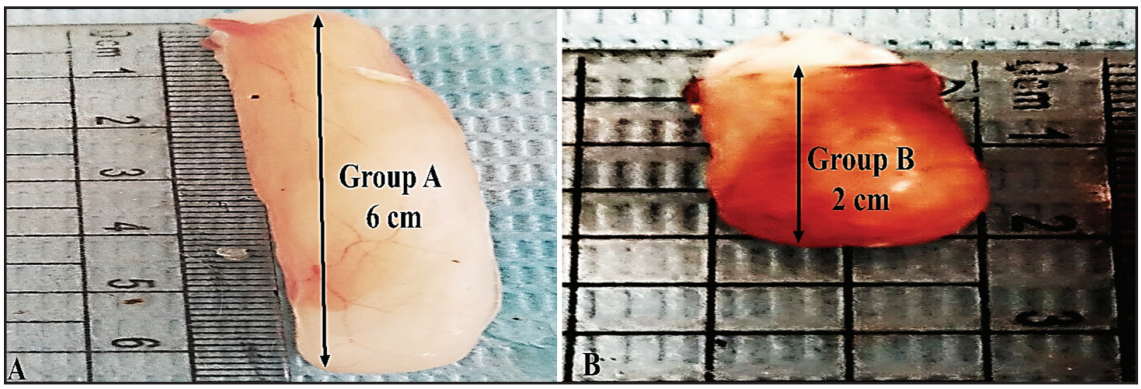

Fig. (1) Gross appearance of buccal pouches. (A) Showing the left pouch of hamsters from group A (negative control) measuring 5-6cm. (B) Showing marked shortening of the left pouch in group B (positive control) to about 2 cm with sever inflammation of the distal end.

showed degenerated distal end with severe dysplastic epithelium up to CIS with focal superficial invasion. The lamina propria was thicker and highly inflamed. The muscle layer'bulk showed marked reduction, where MFs were multinucleated and widely separated by loose fatty connective tissue.

Whereas at 7 and 4 days after one and two TQ injection(s), respectively the surface epithelium showed moderate to mild dysplasia with thinner and slightly inflamed lamina propria. The muscle layer bulk was progressively forming. At about 20 days after one and two TQ injection(s), the surface epithelium appeared normal with near normal thickness of muscle layer **(Figures 2 &3)**. Healing of the necrotic distal end was at 14 and 7 days after one and two TQ injection(s), respectively. Whereas the reduction of lamina propria thickness appeared at 4 and 2 days after one and two TQ injection(s), respectively.

Immunohistochemical results:

Perivascular mononuclear cells (MNCs) were seen from days 2 and 1, to 14 and 7 days after one and two TQ injection(s), respectively. Their nuclei were Pax-7 positive. Furthermore, the peripheral nuclei of MFs were Pax-7 positive from 4 and 2 days to about 20 and 14 days after one and two TQ injection(s), respectively **(Figure 4)**.

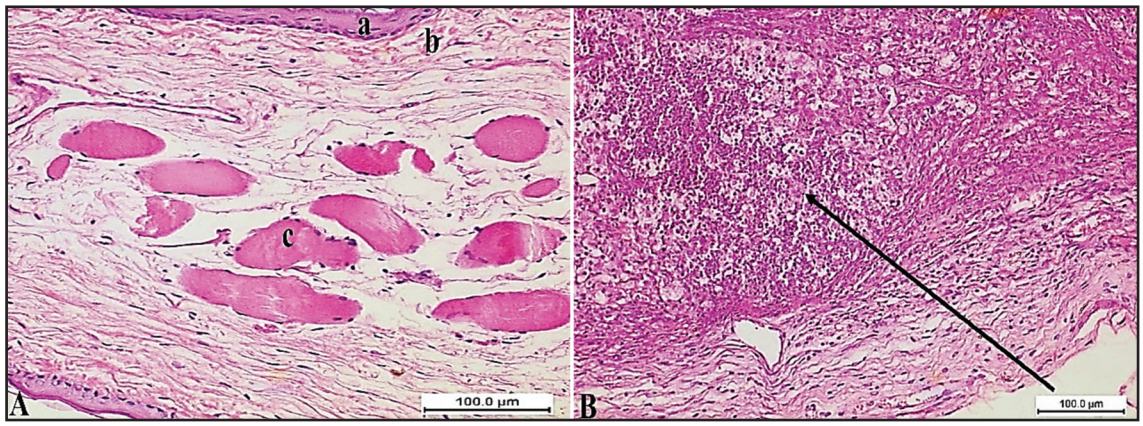

Fig. (2) Photomicrographs of left buccal pouches from negative and positive control groups. (A) Showing normal buccal pouch formed of thin keratinized epithelium (a), collagenous lamina propria (b), and loose muscle layer (c). There are no inflammatory cells. (B) Showing degenerating distal end of the pouch (arrow) with no muscle fibers at this distal end (A and B: H&E X40).

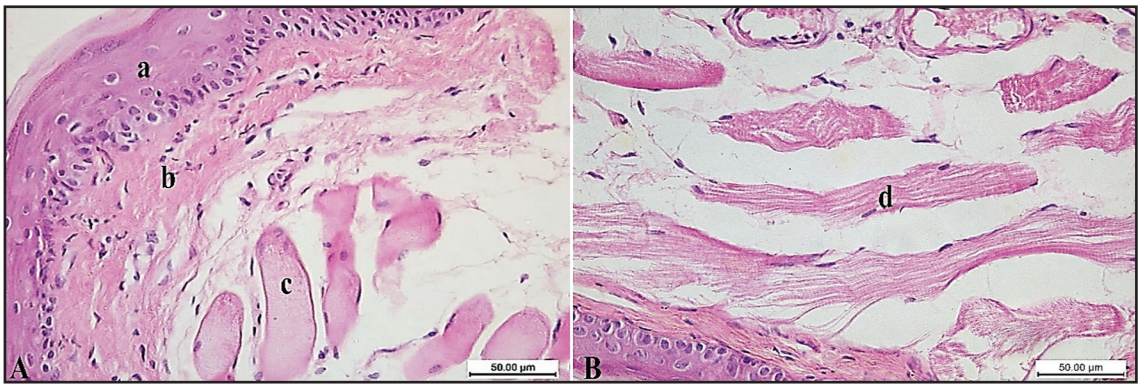

Fig. (3) Photomicrographs of left buccal pouches after TQ injection(s). (A) Showing hyperkeratinised, hyperplastic epithelium (a), thick lamina propria (b) and progressively forming MFs (c) at 4 days after TQ injection(s). (B) Showing normal bulk of the muscle layer (d) at 20 days of TQ injection(s). (A&B: H&EX40).

The IHC stain of NFH in group A was moderate as seen at the MFs membranes' plaques, whereas in group B appeared as mild stain in some MFs membranes' plaques. The intensity of NFH IHC stain was progressively increasing after TQ injection(s) in all experimental groups from 2 and 1 day(s) to 20 days after one and two TQ injection(s), respectively **(Figure 5)**.

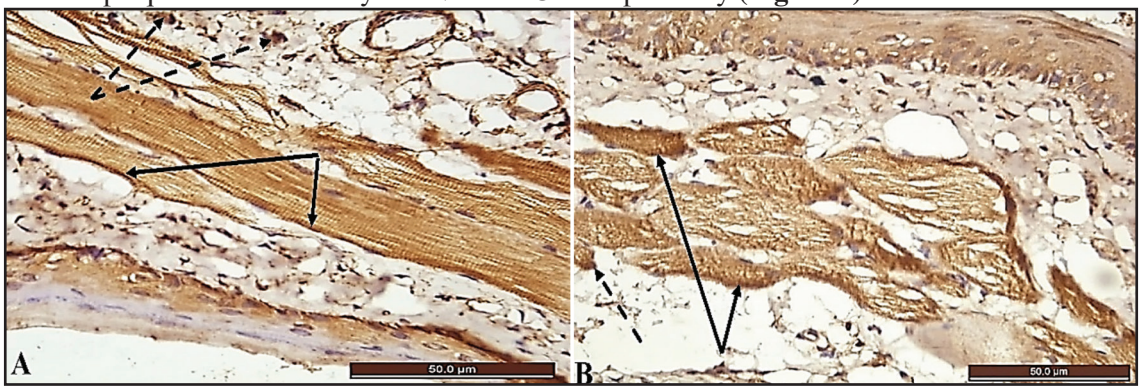

Fig. (4) Photomicrographs of sections from left pouches after one and two TQ injection(s). (A) Showing the perivascular MNCs (dotted arrows) and the peripheral MFs nuclei (arrows) that were Pax-7 positive at 4 days after one TQ injection. (B) Showing the perivascular MNCs (dotted arrow) and the peripheral MFs nuclei (arrow) that were Pax-7 positive at 2 days after two TQ injections (A&B: Pax-7 ABC-DABX40).

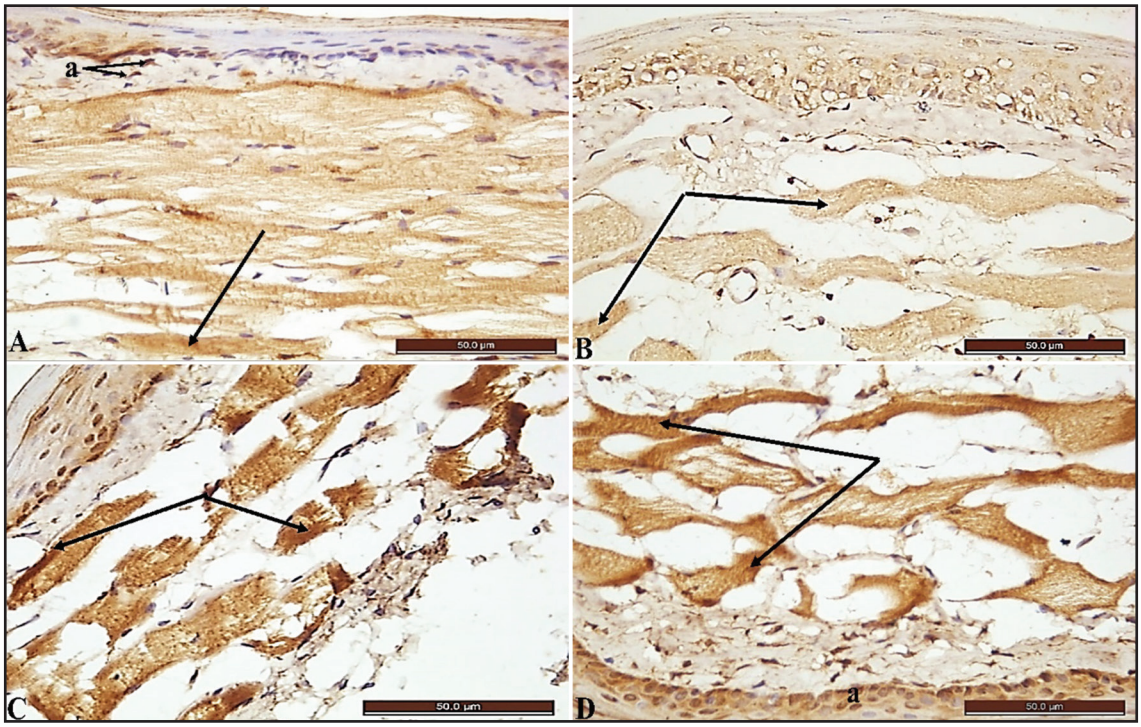

Fig. (5) Photomicrographs of immunohistochemistry-stained sections of left buccal pouches. (A): Showing moderate diffuse stain of fibroblasts (a), MFs'membranous plaques (arrows) in negative control group. (B) Showing mild diffuse stain of MFs' cytoplasm (arrows) in the positive control group. (C) Showing increasing NFH IHC stain intensity of MFs and their membranes' plaques (arrows) at 20 days after one TQ injection. (D): Showing increased NFH stain intensity of basal epithelial cells (a), MFs' cytoplasm and their membranes' plaques (arrows) at 20 days after two TQ injections (A-D: NFH ABC-DAB×40).

Statistical analysis of IHC stain intensity:

The mean difference of IHC stain intensity between subgroups was significant at p value of ≤0.05. There was no significant difference of IHC stain intensity of Pax-7 between the negative control group (group A) and the positive control group (group B). Whereas in group CI, the intensity of Pax-7 started to increase significantly from two days after one TQ injection and reached the peak at seven days after one TQ injection. Pax-7 then started to decrease gradually till reaching twenty days after one injection **(Table 1)**. While in group CII, Pax-7 showed significant increase at one day after two TQ injections when compared with both groups A and B. It reached the peak at four days after two injections then its intensity started to decrease till twenty days **(Table 3)**.

On the other hand, the IHC stain intensity of NFH showed significant decrease in group B (positive control group) when compared with group A (negative control group). The intensity of NFH started to increase gradually and significantly after TQ treatment in both groups CI and CII. It reached the peak at twenty days after one and two TQ injection(s), respectively (**Tables 2 and 4)**.

Table (1) *Results of Pax-7 immunohistochemical stain intensity of all CI (one TQ injection) subgroups, compared to both group A (negative control) and group B (positive control).*

Groups	Mean ± standard deviation	Significance at different times of euthanization							
		G A	G B	1 Day	2 Days	4 Days	7 Days	14 Days	20 Days
Group A	24.2±1.78		1	1	.00*	.00*	.00*	.00*	.00*
Group B	23.06±1.14	1		.99	.00*	.00*	.00*	.00*	.00*
CI (1 day)	25.8±1.1	1	.99		.00*	.00*	.00*	.00*	.00*
CI (2 days)	66.6±6.6	.00*	.00*	.00*		.00*	.00*	.00*	.57
CI (4 days)	111.4±2.5	.00*	.00*	.00*	.00*		.00*	.00*	.00*
CI (7 days)	126.5±1.89	.00*	.00*	.00*	.00*	.00*		.00*	.00*
CI (14 days)	79.09±1.96	.00*	.00*	.00*	.00*	.00*	.00*		.29
CI (20 days)	72.3±4.16	.00*	.00*	.00*	.57	.00*	.00*	.29	

(*) The mean difference was significant at p≤0.05.

Table (2) *Results of NFH immunohistochemical stain intensity of all CI (one TQ injection) subgroups, compared to both group A (negative control) and group B (positive control).*

Groups	Mean ± standard deviation	Significance at different times of euthanization							
		G A	G B	1 Day	2 Day	4 Days	7 Day	14 Day	20 Day
Group A	121±4.9		.00*	.00*	.00*	.00*	1	.12	.01*
Group B	77.4±3.37	.00*		.00*	.00*	.00*	.00*	.00*	.00*
CI (1 day)	86.8±3.8	.00*	.00*		.01*	.00*	.00*	.00*	.00*
CI (2 days)	93.9±3.9	.00*	.00*	.01*		.00*	.00*	.00*	.00*
CI (4 days)	107.9±3.3	.00*	.00*	.00*	.00*		.00*	.00*	.00*
CI (7 days)	120.9±2.04	1	.00*	.00*	.00*	.00*		.09	.01*
CI (14 days)	126.2±1.4	.12	.00*	.00*	.00*	.00*	.09		.99
CI (20 days)	127.8±1.5	.01*	.00*	.00*	.00*	.00*	.01*	.99	

(*) The mean difference was significant at p≤0.05.

Table (3) *Results of Pax-7 immunohistochemical stain intensity of all CII (two TQ injections) subgroups, compared to both group A (negative control) and group B (positive control).*

Groups	Mean ± standard deviation	Significance at different times of euthanization							
		G A	G B	1 Day	2 Day	4 Days	7 Day	14 Day	20 Day
Group A	24.2±1.78		1	.00*	.00*	.00*	.00*	.00*	.00*
Group B	23±1.14	1		.00*	.00*	.00*	.00*	.00*	.00*
CII (1 day)	70.2±3.3	.00*	.00*		.00*	.00*	.00*	.00*	.00*
CII (2 days)	111.5±2.8	.00*	.00*	.00*		.00*	.04*	.00*	.00*
CII (4 days)	123.9±0.91	.00*	.00*	.00*	.00*		.60	.00*	.00*
CII (7 days)	116.2±2.75	.00*	.04*	.00*	.00*	.60		.00*	.00*
CII (14 days)	92.6±3.04	.00*	.00*	.00*	.00*	.00*	.00*		.00*
CII (20 days)	35±3.9	.00*	.00*	.00*	.00*	.00*	.00*	.00*	

(*) The mean difference was significant at p≤0.05.

Table (4) *Results of NFH immunohistochemical stain intensity of all CII (two TQ injections) subgroups, compared to both group A (negative control) and group B (positive control).*

Groups	Mean ± standard deviation	Significance at different times of euthanization							
		G A	G B	1 Day	2 Day	4 Days	7 Day	14 Day	20 Day
Group A	121±4.9		.00*	.00*	.00*	.95	.76	.00*	.00*
Group B	77.4±3.37	.00*		.00*	.00*	.00*	.00*	.00*	.00*
CII (1 day)	94.6±4.6	.00*	.00*		.00*	.00*	.00*	.00*	.00*
CII (2 days)	109.8±2.1	.00*	.00*	.00*		.00*	.00*	.00*	.00*
CII (4 days)	118.9±1.78	.95	.00*	.00*	.00*		.09	.00*	.00*
CII (7 days)	124±1.76	.76	.00*	.00*	.00*	.09		.29	.00*
CII (14 days)	128.2±1.12	.00*	.00*	.00*	.00*	.00*	.29		.03*
CII (20 days)	134±1.9	.00*	.00*	.00*	.00*	.00*	.00*	.03*	

(*) The mean difference was significant at p≤0.05.

DISCUSSION

The HBP/DMBA carcinogenesis model has been used successfully for studying oral squamous cell carcinoma-induction and prevention using different phytochemicals and classic chemotherapy[20-23]. This work used very small concentration of TQ i.p injection (0.1 mg/kg body weight) in hamsters to find out the effect on muscle regeneration and re-innervation following sustained DMBA painting for 6 weeks. Another comparable study carried out in the present lab, reported elongation of the painted HBPs to near normal with malignancy regression[14].

The classic pathway entails activation of satellite cells (SCs) to form multinucleated myotubes, followed by regeneration, differentiation and growth, depending on the inflammatory microienvironment[24]. During muscle regeneration, each phase is coupled to changes in the expression of myogenic transcription factors and their master regulatory genes[3]. In particular Pax-7 is required to maintain the proper myogenic function of satellite cells throughout life[25].

The first point in the present study was the assessment of both right and left hamsters buccal pouches length. In group A, both buccal pouches, and the right pouches of other experimental groups, measured about 5-6 cm and were normal appearing.On the other hand, the left pouches of group B (positive contrrol), showed marked length reduction to about 2 cm, with severe inflammation and necrosis at their distal ends. Comparable findings were reported in previous studies from the present lab that used the same model [13, 14, 26]. Together with the present results, animals received TQ i.p injections after sustained DMBA painting showed gradual elongation of pouches' length with no ulceration or inflammation, as well as regressed epithelial dysplasia to normal appearing epithelium.

The untreated pouches in group A, were normal appearing histopathologically with negative Pax-7 staining of MFs. There was no statistically significant difference of Pax-7 IHC stain intensity between the negative control group (group A) compared with the positive control group (B) (**Table 1**). This results could be due to presence of mature and differentiated MFs (peripherally located nuclei).

The necrosis of DMBA painted pouches in group B, is the most important early change that led to their shortening.These short pouches fail to elongate with progression of malignant process from severe dysplasia to squamous cell carcinoma even after sustained DMBA application. [13, 14, 26] No muscle fibers (MFs) at the necrotic end with increased fat-rich tissue in place of the degenerated muscle layer. Toward the mesial end, the MFs were multinucleated and more loosely arranged than in group A, the epithelium was hyperplastic, hyper-keratinized, with thick collagenous highly inflamed lamina propria. Comparable results were reported in previous studies from this lab [13-15, 27].

The presence of multinucleated MFs (in group B) could be due to the chronic inflammatory environment (DMBA painting) with injured muscles. Inflammatory mediators as tumor necrosis factor- α (TNF-α) synthesized and secreted by neutrophils and macrophages, would activate the quiescent SCs to enter the cell cycle[28]. These multinucleated cells were MyoD negative in a previous study [15] and Pax-7 negative in the present study, that may be due to Pax-7 silence by polycomb repressor complex (PRC2) via inflammation-activated p38 signaling[29,30].

The activated macrophages, neutrophils, mast cells, lymphocytes, eosinophils and muscle fibers (MFs) produce TNF-α, leading to an acute phase of systemic inflammation [30]. The serum TNF-α in the previous study, showed statistically significant difference between positive and negative control groups. The authors explained this significant elevation of serum TNF-α after topical DMBA application to be due to the systemic toxic effect of DMBA. It was highly elevated at early time after one TQ i.p. injection and gradually decreased to near normal at 2 weeks after two TQ injections [15]. It appears that TNF-α was excreted from affected cells to the serum at early times, then gradually decreased to the DMBA-only group level following TQ injection. Another study reported the negative IHC stain of TNF-α in both inflammatory and epithelial cells (of DMBA painted pouches), whereas the inflammatory cells were extruded from pouches' lining after TQ injection(s) [14].

After TQ treatment, the epithelium showed moderate dysplasia at 2 and 1 day(s) to normal appearing epithelium at 14 and 7 days after 1 and 2 TQ injection(s), respectively. The heeling of necrotic distal end was at 14 and 7 days after one and two TQ injection(s), respectively. These finndings indicate the cumulative effect of the used low concentration of TQ., i.e TQ has anti-carcinogenic and anti-inflammatory effects.

After 1 day of 1 and 2 TQ injection(s), the pouches showed no MFs at the necrotic end. Moreover, MFs towards the mesial end showed negative Pax-7 IHC stain. These findings contradict Chen *et al*. report where stimulation of stem (satellite) cells starts 4 hours post-injury as a classic sequence of muscle regeneration. [31] Within the first day after muscle injury, the increased number of neutrophils and macrophages with the inflammatory mediators as TNF-α and interferon gamma (IFN-γ) [32]. The TNF-α was found to activate p38α kinase that lead to formation of repressive chromatin on Pax-7 promoter [33].

The muscle bulk layer was progressively forming from 7 and 4 days after 1 and 2 TQ injection(s). The inflammatory cells showed focal aggregation under the surface epithelium at 7and 2 days after one and two TQ injection(s), respectively. This was online with Hassan *et al*. and Algharyni *et al*. results, that revealed focal accumulation of the inflammatory cells, then their expulsion from the surface epithelium after TQ treatment [14, 15]. This inflammatory cell expulsion led to decreased inflammatory cytokines as TNF-α. It was reported that loss of TNF-α in acutely injured muscle represses p38 i.e., mitogen-activated protein kinase signals, at 3 days post injury, at muscle stem cells (MSCs) transition from the proliferation to differentiation phases of myogenesis. Moreover, TNF-α was found to activate NF-kB that is important for the function and homeostasis of satellite cells [34]. Hassan *et al*. reported that the absence of local inflammatory cells with negative IHC expression of TNF-α and NF-ϰB, were related to negative Myo-D expression in regenerated mature MFs, while MNCs were positive for Myo-D, in the TQ injected groups [14].

The mononucleated cells (MNCs) were around blood vessles from 2 to near 14 days and from 1 to 7 days after 1 and 2 TQ injection(s), respictevely. Their nuclei were Pax-7 positive. Seale *et al*, explained that their origin to be mononucleated myogenic precursors (satellite cells), that were reactivated by de-innervation, in response to direct muscle trauma or in dystrophies [7]. Mastroyiannopoulos *et al*. reported that myogenin down-regulation (one of the myogenic regulatory factors), in terminally differentiated mouse myotubes induces cellular cleavage into mononucleated cells and cell cycle re-entry [35]. The induced dedifferentiation in multinucleated primary mouse myotubes were found to express genes of embryonic muscle progenitor cells as Myf5, Pax3, and Pax-7, that have the ability to be proliferating mononuclear cells. Moreover, they were able to generate a large number of myofibers after transplantation into a degenerating muscle [36]. They were proposed to be the origin of deeply new MFs. Moreover, their presence around BV indicated that their origin could be from bone marrow derived- stem cells (BMDSCs), pericytes or de-differentiated muscle satellite cells [36-38].

The peripheral nuclei of MFs were Pax-7 positive from 4 to 20 days and from 2 to 14 days after 1 and 2 TQ injecion(s), respictively. This indicated the activation of satellite cells during their proliferation from 4 and 2 days after one and two TQ injection(s), respectively. Also, during their differentiation and maturation at 20 and 14 days after one and two TQ injection(s), respectively. The MFs showed negative Pax-7 IHC stain, at 20 days after 2 TQ injections i.e during the functional recovery phase of myogenesis [5, 6]. Following activation of satellite cells, *Pax-7* is activated then progressively became transcriptionally inactive in most satellite cell progeny as they committed to differentiation [39]. This switch of Pax-7 expression represents the formative state (Pax-7 positive) to the remodeling and functional states (Pax-7 negative).

In the present study a fat-rich zone around the necrotic end, was found in all experimental groups in early time interval, i.e. muscle degeneration and early healing of MFs. New MFs noted between this fat rich tissue up to day 14 after TQ injection(s), i.e. after complete healing of the necrotic area [25, 30]. This indicated activation of fibro-adipogenic cells (FAPs) to form new MFs [40]. The previous study from this lab, used Masson's trichrome stain and proved that under TQ effect, there were transition from fibrotic to myogenic differentiation in the area near necrosis [14]. It was also reported that adipose tissue derived mesenchymal stem cells (AT-MSCs) contribute to myo-regeneration and considered more efficient than bone marrow derived stem cells (BMDSCs) and synovial stem cells (SM-SCs) [41].

The interactions between muscle progenitor cells, inflammatory cells and fibro-adipogenic cells (FAPs) are a source of signals inducing differentiation of primary myoblasts [42]. Accumulation of FAPs during chronic inflammation is responsible for fibrosis of the injured muscles [43]. In normal state, FAPs interact with the surrounding microenvironment to proliferate and differentiate to either lipogenic or fibrogenic lineage. Previous study reported that during chronic muscle injury, macrophages secrete high levels of TGF-β1, that would antagonize the TNF-mediated apoptosis of FAPs and induce their fibrogenic differentiation [44]. The used concentration and route of administration of TQ, in this study, appeared to stimulate FAPs' proliferation in response to muscle injury to transiently enhance myogenic differentiation. This result is comparable with previous studies carried out in this lab[14,15,27]. These studies pointed out that local depletion of TNF-α had changed the local microenvironment towards myogenic differentiation of non-myogenic cells as FAPs, MNCs, and fibroblasts of the lamina propria.

The reduction of the lamina propria thickness from day 4 after one TQ injection indicated that the superficially formed MFs were mediated by transition of lamina propria' fibroblasts to the myogenic lineage [42, 45]. Whereas the deeper MFs were formed through MNCs that may be bone marrow derived cells (BMDSCs), pericytes [38, 46] or activated satellite cells [35, 36]. These results are consistent with Hassan *et al*. and Algharyni *et al*., who demonstrated reduction of lamina propria thickness with progression of MFs' formation [14, 15]. Hassan *et al*, reported transition from fibrotic to myogenic lineage by Masson's trichome stain [14].

The intensity of Pax-7 stain was online with the classic frame of Pax-7 expression following muscle injury (3 days) [31]. In group CI, the intensity of Pax-7 was significantly increased from 2 days after one TQ injection and reached the peak at 7 days. Followed by steady decrease till 20 days. There were significant differences when comparing both groups A and B with 2,4,7,14, and 20 days subgroups. Group CII showed statitically significant increase of PAX-7at 1 day after two TQ injections when compared with both groups A and B. It reached the peak at 4 days, then started to decrease till 20 days, where there were significant differences when comparing both groups A and B with 1,2,4,7,14,and 20 days subgroups.

The results of the present study demonstrated the necrotic phase extended for 2 and 1 days after one and two TQ injection(s), respectively. As well as the inflammatory phase appeared up to 7 and 2 days after one and two TQ injection(s), respectively. The MFs were progressively forming along the pouches length, from 7 and 4 days after one and two TQ injection(s), respectively, and up to 20 days where the maturation, remodelling and functional restoration started. These results slightly different with the results of Musarò,and Forcina *et al*., i.e. the classic models of muscle regeneration [5, 6]. These may be due to the difference of muscle injury induction in the present study by DMBA compared to CTX injection in previous studies, or due to different animal models (hamsters cheek pouch in the present work or rats and mice tibialis muscle in previous work) in the previous study) or due to different type of muscle (this work used HBPs that were considered to be afree end muscle). Two TQ injections resulted in expulsion of inflammatory cells at second day of last injection, new MFs were progressively forming from the 4th day, complete restoration of muscle bulk was at 14th day and complete remodeling and maturation was at 20th day after last TQ injection. The present study proved the cumulative anti-inflammatory, anti-carcinogenic and myogenic effects of the used two TQ injections.

This study used the NFH IHC stain as a marker of peripheral motor nerve alteration during the experiment. In group A (negative control group), NFH showed moderate stain of MFs membranes' plaques, this result supported the functions of NFs. NFs are group of cytoskeleton proteins that form and maintain nerve shape and facilitate the transport of particles and organelles within the cytoplasm [9].

In group B (positive control group), NFH showed mild expression of some MFsmembranes' plaques. In previous study, it was reported that after peripheral nerve injuries, the nerve axon distal to injury site, remain intact for some days before granular disintegration of the cytoskeleton [47]. The mean NFH intensity in group B showed statistically significant differences when compared with groups A, all CI and CII subgroups.

The mild NFH expresion of focal membranous' plaques after one day of 1 TQ injection, could be due to injury of nerves induced by DMBA painting [48, 49]. This mild expression could be due to the delayed phosphorylation and axon transport of the NFH, as it was reported that more extensive phosphorylation of NFM and NFH is delayed until newly formed NFs have translocated into axons [50]. Moreover, during nerve regeneration, NFs reemerge in a sequence resembling that during development of neurons, this could be the reason of presence of positive focal membranous' plaques [51]. It was reported that the expression of NFL and NFM during postnatal development is before NFH [52].

There were increasing NFH stain intensity from 2 and 1 day(s) to 20 days after one and two TQ injection(s), respectively. These findings were due to the progressive formation of new nerves, as reported in previous studies [51-53]. These findings indicated the cumulative effect of two TQ injections, as TQ has many neuroprotective effects through its antioxidant, anti-inflammatory effects with inhibition of lipid peroxidation-inflammatory mediators production [54].

The interesting finding that the surface epithelium was Pax-7 and NFH positive in groups B, early points of follow up in CI and CII. These findings can be explained due to returning the tissue to an embryonal-like state by the induced dysplasia, so this dysplastic tissue expresses many genes, and their expression decreases after regaining normal phenotype. After TQ treatment, the stain intensity became faint to negative mostly due to the reduced toxic microenvironment of DMBA and regression of severe dysplasia to normal appearing epithelium.

CONCLUSIONS

- The muscle regeneration in this chemically induced carcinogenesis model, appears different than the classic models of muscle regeneration, where the activated satellite cells did not take the upper hand.
- FAPs from the fat rich area at distal end are involved in the regeneration process, at least for elongation of the short pouches at the distal end.
- The muscle regeneration in this model takes place by perivascular MNCs (the deeper layer) and fibroblasts of lamina propria at the upper side. Both were Pax-7 positive along the follow up time after TQ in groups CI and CII till end of the proliferation phase.
- The nerve regeneration in this model follows MFs formation and maturation as shown by NFH expression that was decreased after DMBA application due to nerve and muscle necrosis. Then, gradually increased as during development till reaching the threshold level, at which the expression declines by dephosphorylation and subsequent proteasomal degradation.

RECOMMENDATIONS

From the present results it can be recommended to try higher doses and other routes of administration of TQ and other models of muscle and nerve injury. As well as testing muscle function restoration after TQ treatment using specific techniques as electromyography.

ACKNOWLEDGMENT

We would like to thank all Oral Pathology Department staff members for their tireless efforts.

REFERENCES

1. Juhas M, Bursac N. Engineering skeletal muscle repair. Curr Opin Biotechnol. 2013; 24: 880-886. https://doi.org/10.1016/j.copbio.2013.04.013.
2. Gayraud-Morel B, Chrétien F, Tajbakhsh S. Skeletal muscle as a paradigm for regenerative biology and medicine. Regen Med. 2009; 4: 293-319. https://doi.org/10.2217/17460751.4.2.293.
3. Chargé SB, Rudnicki MA. Cellular and molecular regulation of muscle regeneration. Physiol Rev. 2004; 84: 209-238. http://doi.org/10.1152/physrev.00019.
4. Schiaffino S, Dyar KA, Ciciliot S, Blaauw B, Sandri M. Mechanisms regulating skeletal muscle growth and atrophy. FEBS J. 2013; 280: 4294-4314. https://doi.org/10.1111/febs.12253.
5. Musarò A. The Basis of Muscle Regeneration. Adv Biol. 2014; 2014: 1-16. https://doi.org/10.1155/2014/612471.
6. Forcina L, Cosentino M, Musarò A. Mechanisms regulating muscle regeneration: Insights into the interrelated and time-dependent phases of tissue healing. Cell. 2020; 9: 1297-1325. https://doi.org/10.3390/cells9051297.
7. Seale P, Sabourin L, Girgis-Gabardo A, Mansouri A, Gruss P, Rudnicki M. Pax7 is required for the specification of myogenic satellite cells. Cell. 2000; 102: 777-786. https://doi.org/10.1016/s0092-8674(00)00066-0.
8. Yum SW, Zhang J, Mo K, Li J, Scherer SS. A novel recessive NEFL mutation causes a severe, early-onset axonal neuropathy. Ann Neurol. 2009; 66: 759-770. https://doi.org/10.1002/ana.21728.
9. Liu Q, Xie F, Siedlak S, Nunomura A, Honda K, Moreira PI, Zhua X, Smith M, Perry G. Neurofilament proteins in neurodegenerative diseases. Cell Molec Life Sci. 2004; 61: 3057-3075. https:///doi.org/10.1007/s00018-004-4268-8.
10. Darabid H, Perez-Gonzalez AP, Robitaille R. Neuromuscular synaptogenesis: coordinating partners with multiple functions. Nat Rev Neurosci. 2014; 15: 703-718.
11. Shklar G. Development of experimental oral carcinogenesis and its impact on current oral cancer resecuch. J Dent Res. 1999; 78: 1768-1772. https://doi.org/10.1177/00220345990780120101.
12. Woo C, Kumar A, Sethi G, Tan K. Thymoquinone: potential cure for inflammatory disorders and cancer. Biochem Pharmacol. 2012; 83: 443-451. https://doi.org/10.1016/j.bcp.2011.09.029.
13. El-Khoriby S. Chemo preventive effect of different doses of nano-thymoquinone on chemically-induced oral carcinogenesis Thesis. Egypt: Suez Canal University; 2015.
14. Hassan M, Abdel-Latif G, El-Hossary W. Protective and promising myogenic effect of two thymoquinone formulations in relation to the pouch-induced carcinogenic model. J Dent Med Sci 2017; 16: 54-66. https://doi.org/10.9790/0853-1605035466.
15. Algharyni HM, El-Hossary WH, Korraah AM, Hassan MM. Expression of MyoD in the DMBA-treated hamster pouches following thymoquinone injection. J Dent Med Sci 2019; 18: 35-40. https://doi.org/:10.9790/0853-1802043540.
16. Erkut A, Cure M, Kalkan Y, Balik M, Guvercin Y, Yaprak E, Yuce S, Sehitoglu I, Cure E. Protective effects of thymoquinone and alpha-tocopherol on the sciatic nerve and femoral muscle due to lower limb ischemia-reperfusion injury. Eur Rev Med Pharmacol Sci. 2016; 20: 1192-1202.
17. Bánóczy J, Csiba Á. Occurrence of epithelial dysplasia in oral leukoplakia: analysis and follow-up study of 12 cases. Oral Surg Oral Med Oral Pathol. 1976; 42: 766-774. https://doi.org/10.1016/0030-4220(76)90099-2.
18. Mane DR, Kale AD, Belaldavar C. Validation of immunoexpression of tenascin-C in oral precancerous and cancerous tissues using ImageJ analysis with novel immuno-

histochemistry profiler plugin: An immunohistochemical quantitative analysis. J Oral Maxillofac Pathol. 2017; 21: 211-217. https://doi.org/10.4103/jomfp.JOMFP_234_16.

19. Field A. Discovering statistics with SPSS for Windows. London: Sage; 2000.
20. AL-Jawfi K, Hassan M, El-Gohary A. Effect of Nigella sativa oil on the hamster lymphocytes secondary to DMBA-induced carcinogenesis. Suez Canal Med J. 2008; 11: 75-80.
21. El-Dakhakhny M, Hassan M, Abd El-Aziz G. Effect of thymoquinone and polythymoqunione on chemically-induced oral epithelial dysplasia (experimental study) (Part I). Int J Ac Res. 2009; 1: 107-117.
22. Hassan M, El-Dakhakhny M. Effect of some Nigella sativa constituents on chemical carcinogenesis in hamster cheek pouch'. J Egypt Soc Pharmacol ExpTher. 1992; 11: 675–677.
23. Rajkamal G, Suresh K, Sugunadevi G, Vijayaanand M, Rajalingam K. Evaluation of chemopreventive effects of Thymoquinone on cell surface glycoconjugates and cytokeratin expression during DMBA induced hamster buccal pouch carcinogenesis. Biochem Molec Biol Rep. 2010; 43: 664-669. https://doi.org/10.5483/BMBRep.2010.43.10.664.
24. Aziz A, Sebastian S, Dilworth FJ. The origin and fate of muscle satellite cells. Stem Cell Rev Rep. 2012; 8: 609-622. 10.1007/s12015-012-9352-0.
25. Wang YX, Dumont NA, Rudnicki MA. Muscle stem cells at a glance. J Cell Sci. 2014; 127: 4543-4548. https://doi.org/10.1242/jcs.151209.
26. El-Sherbiny RH, Hassan MM, Korraah AM. Effect of different nanothymoquinone concentrations on the chemically-induced epithelial dysplasia in the hamster buccal pouch. Suez Canal Univ Med J. 2017; 20: 75-88.
27. Hassan M, El-Hossary W, Hanafi R. Anti-inflammatory Thymoquinone and Muscle Regeneration in the Hamster Buccal Pouch-Induced Dysplasia. J Oral Health Dent Sci. 2020; 3: 1-14.
28. Bossola M, Marzetti E, Rosa F, Pacelli F. Skeletal muscle regeneration in cancer cachexia. Clin Exp Pharmacol Physiol. 2016; 43: 522-527. https://doi.org/10.1111/1440-1681.12559.
29. Bracken AP, Dietrich N, Pasini D, Hansen KH, Helin K. Genome-wide mapping of Polycomb target genes unravels their roles in cell fate transitions. Genes Dev. 2006; 20: 1123-1136. https://doi.org/10.1101/gad.381706.
30. Lee TI, Jenner RG, Boyer LA, Guenther MG, Levine SS, Kumar RM, Chevalier B, Johnstone SE, Cole MF, Isono K-i. Control of developmental regulators by Polycomb in human embryonic stem cells. Cell. 2006; 125: 301-313. https://doi.org/10.1016/j.cell.2006.02.043.
31. Chen S-E, Jin B, Li Y-P. TNF-alpha regulates myogenesis and muscle regeneration by activating p38 MAPK. American Journal of Physiology. Cell Physiol. 2007; 292: C1660-C1671. https://doi.org/10.1152/ajpcell.00486.2006.
32. Torrente Y, El Fahime E, Caron N, Del Bo R, Belicchi M, Pisati F, Tremblay J, Bresolin N. Tumor necrosis factor-α (TNF-α) stimulates chemotactic response in mouse myogenic cells. Cell transplant. 2003; 12: 91-100. https://doi.org/10.3727/000000003783985115.
33. Palacios D, Mozzetta C, Consalvi S, Caretti G, Saccone V, Proserpio V, Marquez VE, Valente S, Mai A, Forcales SV, Sartorelli V, Puri PL. TNF/p38α/polycomb signaling to Pax7 locus in satellite cells links inflammation to the epigenetic control of muscle regeneration. Cell. 2010; 7: 455-469. https://doi.org/10.1016/j.stem.2010.08.013.
34. Wulan SMM, Laswati H, Purnomo W, Pangkahila A, Nasronudin N, Hadi U. Tumor Necrosis Factor Alpha (TNF-α), Nuclear Factor of kappa B (NF-kB) p65 and calcineurin expression play a role in the regulation of muscle regeneration process through aerobic exercise in HIV patients. Bali Med J. 2017; 6: 421-426. https://doi.org/10.15562/bmj.v6i2i.607.
35. Mastroyiannopoulos NP, Nicolaou P, Anayasa M, Uney JB, Phylactou LA. Down-regulation of myogenin can reverse terminal muscle cell differentiation. PLoS One. 2012; 7: e29896. https://doi.org/10.1371/journal.pone.0029896.
36. Yang Z, Liu Q, Mannix RJ, Xu X, Li H, Ma Z, Ingber DE, Allen PD, Wang Y. Mononuclear cells from dedifferentiation of mouse myotubes display remarkable regenerative capability.Cell. 2014; 32: 2492-2501. https://doi.org/10.1002/stem.1742.
37. Bentzinger CF, von Maltzahn J, Dumont NA, Stark DA, Wang YX, Nhan K, Frenette J, Cornelison D, Rudnicki MA. Wnt7a stimulates myogenic stem cell motility and engraftment resulting in improved muscle strength. J Cell Biol. 2014; 205: 97-111. https://doi.org/10.1083/jcb.201310035

38. Kostallari E, Baba-Amer Y, Alonso-Martin S, Ngoh P, Relaix F, Lafuste P, Gherardi RK. Pericytes in the myovascular niche promote post-natal myofiber growth and satellite cell quiescence. Dev. 2015; 142: 1242-1253. https://doi.org/10.1242/dev.115386

39. Zammit P, Relaix F, Nagata Y, Ruiz A, Collins C, Partridge T, Beauchamp J. Pax7 and myogenic progression in skeletal muscle satellite cells. J Cell Sci. 2006; 119: 1824-1832. https://doi.org/10.1242/jcs.02908.

40. Lemos DR, Babaeijandaghi F, Low M, Chang C-K, Lee ST, Fiore D, Zhang R-H, Natarajan A, Nedospasov SA, Rossi FM. Nilotinib reduces muscle fibrosis in chronic muscle injury by promoting TNF-mediated apoptosis of fibro/adipogenic progenitors. Nat Med. 2015; 21: 786-794. https://doi.org/10.1038/nm.3869. .

41. De La Garza-Rodea AS, Van Der Velde-Van Dijke I, Boersma H, Gonçalves MA, Van Bekkum DW, De Vries AA, Knaän-Shanzer S. Myogenic properties of human mesenchymal stem cells derived from three different sources. Cell Transplant. 2012; 21: 153-173. https://doi.org/10.3727/096368911X580554.

42. Joe AWB, Yi L, Natarajan A, Le Grand F, So L, Wang J, Rudnicki MA, Rossi FM. Muscle injury activates resident fibro/adipogenic progenitors that facilitate myogenesis. Nat Cell Biol. 2010; 12: 153-163. https://doi.org/10.1038/ncb2015.

43. Rebolledo D, González D, Faundez-Contreras J, Contreras O, Vio C, Murphy-Ullrich J, Lipson K, Brandan E. Denervation-induced skeletal muscle fibrosis is mediated by CTGF/CCN2 independently of TGF-β. Matrix Biol. 2019; 82: 20-37. https://doi.org/10.1016/j.matbio.2019.01.002.

44. Juban G, Saclier M, Yacoub-Youssef H, Kernou A, Arnold L, Boisson C, Ben Larbi S, Magnan M, Cuvellier S, Théret M, Petrof B, Desguerre I, Gondin J, Mounier R, Chazaud B. AMPK Activation regulates LTBP4-dependent TGF-β1 secretion by pro-inflammatory macrophages and controls fibrosis in duchenne muscular dystrophy. Cell Rep. 2018; 25: 2163-2176.e2166. https://doi.org/10.1016/j.celrep.2018.10.077.

45. Uezumi A, Fukada S-i, Yamamoto N, Takeda Si, Tsuchida K. Mesenchymal progenitors distinct from satellite cells contribute to ectopic fat cell formation in skeletal muscle. Nat Cell Biol. 2010; 12: 143-152. https://doi.org/10.1038/ncb2014.

46. Torrente Y, Belicchi M, Sampaolesi M, Pisati F, Meregalli M, D'Antona G, Tonlorenzi R, Porretti L, Gavina M, Mamchaoui K, Pellegrino MA, Furling D, Mouly V, Butler-Browne GS, Bottinelli R, Cossu G, Bresolin N. Human circulating AC133+ stem cells restore dystrophin expression and ameliorate function in dystrophic skeletal muscle. J Clin Invest. 2004; 114: 182-195. https://doi.org/10.1172/JCI20325.

47. Stirling D, Stys P. Mechanisms of axonal injury: internodal nanocomplexes and calcium deregulation. Trends Mol Med. 2010; 16: 160-170. https://doi.org/10.1016/j.molmed.2010.02.002.

48. Hoffman P, Pollock S, Striph G. Altered gene expression after optic nerve transection: reduced neurofilament expression as a general response to axonal injury. Exp Neurol. 1993; 119: 32-36. https://doi.org/10.1006/exnr.1993.1004.

49. Yuan A, Sasaki T, Rao MV, Kumar A, Kanumuri V, Dunlop DS, Liem RK, Nixon RA. Neurofilaments form a highly stable stationary cytoskeleton after reaching a critical level in axons. J Neurosci. 2009; 29: 11316-11329. https://doi.org/10.1523/JNEUROSCI.1942-09.2009

50. Nixon RA, Paskevich PA, Sihag RK, Thayer CY. Phosphorylation on carboxyl terminus domains of neurofilament proteins in retinal ganglion cell neurons in vivo: influences on regional neurofilament accumulation, interneurofilament spacing, and axon caliber. J Cell Biol. 1994; 126: 1031-1046. https://doi.org/10.1083/jcb.126.4.1031.

51. Yuan A, Rao M, Veeranna R, Nixon R. Neurofilaments and Neurofilament Proteins in Health and Disease. Cold Spring Harb Perspect Biol. 2017; 9: a018309. https://do.org/10.1101/cshperspect.a018309.

52. Faussone-Pellegrini M-S, Matini P, DeFelici M. The cytoskeleton of the myenteric neurons during murine embryonic life. Anat Embryol. 1999; 199: 459-469. https://doi.org/10.1007/s004290050244.

53. Zhao Y, Szaro B. The optic tract and tectal ablation influence the composition of neurofilaments in regenerating optic axons of Xenopus laevis. J Neurosci. 1995; 15: 4629-4640. https://doi.org/10.1523/JNEUROSCI.15-06-04629.1995

54. Jayasooriya RGPT, Lee K-T, Kang C-H, Dilshara MG, Lee H-J, Choi YH, Choi I-W, Kim G-Y. Isobutyrylshikonin inhibits lipopolysaccharide-induced nitric oxide and prostaglandin E2 production in BV2 microglial cells by suppressing the PI3K/Akt-mediated nuclear transcription factor-ϰB pathway. Nutr Res. 2014; 34: 1111-1119. https://doi.org/10.1016/j.nutres.2014.10.002.